Contribution from the Department of Chemistry, Williams College, Williamstown, Massachusetts 01267, and Gibbs Chemical Laboratory, Harvard University, Cambridge, Massachusetts 02138

Fluxional Behavior in $B_8H_8^{2-}$. A Theoretical Study

DANIEL A. KLEIER[1a] and WILLIAM N. LIPSCOMB*[1b]

Received August 17, 1978

Molecular orbital calculations using the PRDDO approximation are reported for various geometries of $B_8H_8^{2-}$ in order to study its fluxional behavior. A low-energy path with a barrier less than 4 kcal/mol has been found for rearrangement. The low-energy path connects D_{2d} and C_{2v} geometries; the D_{2d} is predicted to be more stable. No computational evidence in support of a stable D_{4d} structure was found. Wave functions and energies are also reported for four additional structures of high symmetry, none of which are energetically competitive with the D_{2d}, C_{2v}, and D_{4d} triumvirate. Environmental factors such as solvation and ion pairing were also considered by using a supermolecule approach. Solvation by hydrogen fluoride was found to have little effect on the relative stabilities of the various structures. Some support for the concept that cations stabilize square faces is found from computations on $Li^+B_8H_8^{2-}$. However, addition of a second Li^+ ion firmly establishes the stability order: $D_{2d} > C_{2v} > D_{4d}$. Correlation diagrams for the $D_{2d} \rightleftarrows C_{2v}$ and $C_{2v} \rightleftarrows D_{4d}$ transformations are constructed. Localized molecular orbitals for the highly symmetric structures are presented and correlations among the LMO's are discussed. Finally the temperature-dependent NMR spectra of the octaborane dianion are given an alternative explanation in the light of our computations.

I. Introduction

Structural nonrigidity has been observed[2,3] for the polyhedral boranes $B_8H_8^{2-}$ and $B_{11}H_{11}^{2-}$. In addition to the intrinsic interest of these rearrangements, they also serve as prototypes for cluster rearrangements in coordination compounds or metal clusters. Recent applications[4] of molecular orbital theory to the rearrangement in $B_{11}H_{11}^{2-}$ have successfully accounted for the nonrigidity in this molecule. We are thus encouraged to extend this procedure to the octaborane dianion.

The solid-state structure of $B_8H_8^{2-}$ is a slightly distorted dodecahedron (D_{2d}).[5,6] There is a suggestion, however, that two different forms are more stable in solution.[2,7] These are the D_{4d} square antiprism and the C_{2v} bicapped trigonal prism (Figure 1). It has been proposed[2,7] that borons are permuted within the C_{2v} form by traversing a D_{2d} intermediate.

Previous theoretical studies of $B_8H_8^{2-}$ have been limited to idealized structures. Extended Hückel calculations have been performed on the idealized structures having D_{4d}, C_{2v}, D_{2d}, O_h, D_{3d}, and D_{3h} symmetry.[6,8,9] Only for the D_{2d} structure have higher quality wave functions been computed.[10]

In this paper we use molecular orbital theory to explore the potential energy surface for $B_8H_8^{2-}$. Computational details are described in section II and the energetics of rearrangement in section III. In section IV the relative stabilities of the various structures are rationalized by an analysis of the corresponding wave functions. Section V deals with possible environmental factors which might influence the relative stabilities of the various structures, and in the final section our results are compared with experiment.

II. Computational Details

The molecular orbital calculations are performed by using the PRDDO approximation[11] which has been demonstrated[12] to mimic closely ab initio computations at the minimum basis set level. The exponents used for the Slater orbitals were those optimized for B_2H_6[13] ($\xi_{1s} = 4.680$, $\xi_{2s} = 1.443$, $\xi_{2p} = 1.477$, and $\xi_H = 1.147$). Localized molecular orbitals (LMO's) are reported for the highly symmetrical structures. The LMO's were determined by using the Boys criterion[14] and the 2×2 procedure suggested by Edmiston and Ruedenberg[15] as described elsewhere.[16] Geometries were optimized by sequentially optimizing bond distances and angles subject to the imposed symmetry restraints and maintaining BH distances at 1.19 Å. For example, 13 modes were used for the D_{2d} structure, 22 modes for the C_{2v} structure, and 6 modes for the D_{4d} structure. Energy changes along reaction pathways joining idealized structures were computed using the synchronous transit procedure.[17]

Table I. Energies of Idealized Structures of $B_8H_8^{2-}$ Relative to D_{2d} Conformation

	energy, kcal/mol	
	PRDDO	EHT[b]
D_{2d}	0.0	0.0
C_{2v}	3.6	−6.0
D_{4d}	36.8	−48.4
D_{6h}	73.1	
D_{3d}	133.4	44.7
D_{3h}	152.7	55.6
O_h	367.0 (421.6)[a]	39.2

[a] Value in parentheses corresponds to wave function whose MO's transform according to irreducible representations of the O_h point group. [b] Reference 6.

III. Energetics of Rearrangement

Table I contains the energies of seven highly symmetrical structures of $B_8H_8^{2-}$. These include the dodecahedron (D_{2d}), square face-bicapped trigonal prism (C_{2v}), square antiprism (D_{4d}), symmetrical bicapped trigonal prism (D_{3h}), symmetrical bicapped trigonal antiprism (D_{3d}), cube (O_h), and hexagonal bipyramid (D_{6h}). All structures have been partially optimized with extensive optimization for the D_{2d}, C_{2v}, D_{4d}, and O_h structures as described above. The optimized coordinates are given in Table II. The predicted stability order from the PRDDO calculations is $D_{2d} > C_{2v} > D_{4d} > D_{6h} > D_{3d} > D_{3h} >> O_h$. For comparison we have included the results of the extended Hückel (EHT) calculations[6,9] which are in considerable disagreement with the PRDDO results. Evidently, the EHT method does not predict as much destabilization upon formation of a square face as does PRDDO. Thus, EHT predicts the D_{4d} structure (two square faces) to be more stable than either the D_{2d} (no square faces) structure or the C_{2v} (one square face) structure, and also predicts the O_h structure (six square faces) to be more stable than the D_{3d} and D_{3h} structures which possess zero and three square faces, respectively.

The PRDDO calculations clearly suggest an extremely nonrigid structure for the octaborane dianion. The D_{2d} and C_{2v} structures are of nearly equal stability and either could serve as a transitional structure[18] for permutation of borons in the other. A linear synchronous pathway[17] (Figure 1, top) shows a practically monotonic increase in energy with only the slightest hint of a barrier (maximum < 1 kcal/mol above the C_{2v} structure) as the 3–6 "bond" is broken (Figure 2) in passing from the D_{2d} to C_{2v} structure. The energy of the C_{2v} structure is about 3 kcal/mol above that of the D_{2d} structure. Electron correlation corrections have not been made but we

0020-1669/79/1318-1312$01.00/0

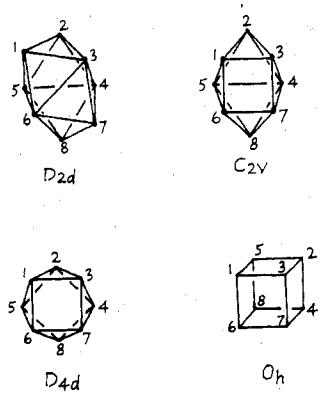

Figure 1. Atomic labels for key idealized structures of $B_8H_8^{2-}$.

Table II. Optimized Coordinates for Symmetrical Structures[a]

structure[b]	atom[c]	x	y	z
D_{2d}	B1 (4)	0.0	1.482 52	2.409 87
	B3 (4)	2.345 61	0.0	0.547 71
	H1 (4)	0.0	2.944 05	4.119 89
	H3 (4)	4.522 61	0.0	1.114 35
C_{2v}	B1 (4)	−1.755 11	1.503 56	2.311 05
	B2 (2)	0.0	2.590 66	0.030 02
	B4 (2)	1.690 61	0.0	−0.739 54
	H1 (4)	−3.182 51	2.831 60	3.433 19
	H2 (2)	0.0	4.645 70	−0.885 78
	H4 (2)	3.283 38	0.0	−2.328 56
D_{4d}	B1 (8)	−1.612 64	1.612 64	1.329 82
	H1 (8)	−2.985 80	2.985 80	2.461 97
D_{3d}	B1 (2)	0.0	0.0	3.574 67
	B2 (6)	0.0	2.040 38	1.421 91
	H1 (2)	0.0	0.0	5.824 67
	H2 (6)	0.0	4.256 86	1.808 86
D_{3h}	B1 (2)	0.0	0.0	3.700 57
	B2 (6)	0.0	2.170 38	1.570 87
	H1 (2)	0.0	0.0	5.950 57
	H2 (6)	0.0	4.225 24	2.487 39
D_{6h}	B1 (2)	0.0	0.0	2.111 40
	B2 (6)	0.0	2.926 53	0.0
	H1 (2)	0.0	0.0	4.361 40
	H2 (6)	0.0	5.176 53	0.0
O_h	B1 (8)	1.690 23	1.690 23	1.690 23
	H1 (8)	2.989 27	2.989 27	2.989 27

[a] All coordinates in au. [b] For the D_{2d}, C_{2v}, D_{4d}, and O_h structures refer to Figure 1. In all cases the principal symmetry axis is collinear with the space-fixed z axis and horizontal symmetry planes are in the xy plane. [c] Number in parentheses gives the number of symmetry related atoms.

guess that they would retain this order of stability and perhaps slightly increase this energy difference.

According to the PRDDO calculations, formation of a second square face in passing from the C_{2v} to the D_{4d} structure is much more energetically demanding than the opening of the first square face in the D_{2d} structure. A comparison of the wave functions for the D_{2d} and C_{2v} structures (section IV) reveals the source of the higher energetic requirements. A linear synchronous transit from the C_{2v} to the D_{4d} structure gives a smooth increase in energy as the 4–5 "bond" is broken; no maximum separates the C_{2v} and D_{4d} structures (Figure 2, top).

The D_{2d} structure of $B_8H_8^{2-}$ can pass into the cubic structure (O_h) conserving D_{2d} symmetry along the entire path. This process is best visualized by observing that the symmetry elements of the cube in Figure 1 are identical with those of the D_{2d} structure if the 1–6 and 2–4 edges of the cube are moved vertically up while the 5–8 and 3–7 edges are moved in the opposite direction. Our PRDDO calculations converged on two different states for the cube depending upon the nature of the starting density matrix. If a standard empirically constructed[11] density matrix is used to initiate the SCF

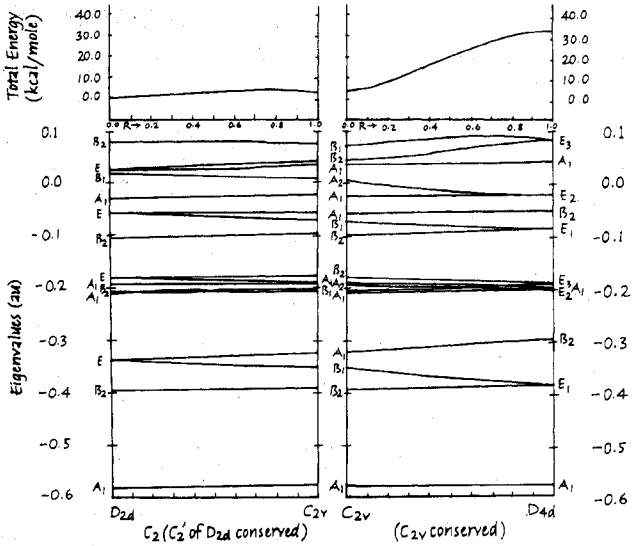

Figure 2. Top: Total energy (kcal/mol) relative to the optimized D_{2d} structure along the linear synchronous transit paths traversing the D_{2d}, C_{2v}, and D_{4d} structures. Bottom: Correlation diagrams for occupied molecular orbitals of D_{2d}, C_{2v}, and D_{4d} structures.

procedure, a state is obtained which lies 421.6 kcal above the most stable structure and the corresponding canonical MO's transform according to irreducible representations of the O_h point group as expected. However, if the initiating density matrix is obtained from a converged calculation for a cube slightly distorted to D_{2d} symmetry, the state obtained is spatially degenerate and about 50 kcal/mol lower in energy but still almost 370 kcal/mol above the ground state of the most stable structure.[19]

Among the remaining structures considered, none appears to be competitive with the D_{2d}, C_{2v}, and D_{4d} triumvirate. The D_{3d} structure is probably more stable than the D_{3h} due to the larger number of square faces in the latter. The D_{6h} structure fares reasonably well because it is completely triangulated, but it suffers due to the unusually high coordination number of the apical borons.

In Table III we present the eigenvalue spectra for the optimized structures of high symmetry. The bottom of Figure 2 is a diagram for the occupied valence orbitals depicting their correlations during the $D_{2d} \rightleftarrows C_{2v}$ and $C_{2v} \rightleftarrows D_{4d}$ transformations. The orbital energies are those computed along the synchronous transit pathways.

In proceeding from the D_{2d} to the C_{2v} structures the common subgroup conserved is C_2. During this rearrangement all valence orbitals correlate smoothly. Only a single crossing of the nearly degenerate orbitals 13 and 14 occurs. No orbital energy changes by more than 11 kcal/mol during this rearrangement and, in particular, the HOMO and HOMO-1 energies change by only 5 and 10 kcal/mol, respectively.

Significantly larger orbital energy changes are observed when a second square is opened during the $C_{2v} \rightleftarrows D_{4d}$ rearrangement. In particular, the largest energy increase (about 25 kcal/mol) occurs for the HOMO-1 of B_2 symmetry. It appears that this orbital is most responsible for the difficulty of opening a second face.

IV. Analysis of Wave Functions

Figure 3 depicts the HOMO-1, HOMO, and LUMO for the D_{2d}, C_{2v}, and D_{4d} structures. These MO's are largely of p-type character and hence only the 2p contributions are indicated for simplicity. In proceeding from the D_{2d} to the C_{2v} structure the p-orbital contributions to the HOMO-1 from borons 4 and 5 pivot to become parallel and hence strengthen the π-bonding interaction between centers 4 and 5. This

Table III. Orbital Energies (au) and Symmetry Types for Valence Orbitals and First Few Virtual Orbitals of Highly Symmetrical Structures

orbital	structure						
	D_{2d}	C_{2v}	D_{4d}	D_{6h}	D_{3d}	D_{3h}	O_h
28	0.762 } (E)	0.806 (A_1)	0.880 (A_1)	0.746 } (E_{1u})	0.700 (A_{1u})	0.709 (A_2')	0.418 } (T_{2u})
27	0.762 }	0.676 (B_1)	0.561 } (E_1)	0.746 }	0.585 } (E_g)	0.591 } (E')	0.418 }
26	0.633 (A_2)	0.600 (B_2)	0.561 }	0.705 } (E_{2u})	0.585 }	0.591 }	0.418 }
25	0.079 (B_2)	0.071 (B_1)	0.084 } (E_3)	0.705 }	0.116 } (E_u)	0.100 } (E'')	0.187 } (T_{2g})
24	0.025 } (E)	0.041 (B_2)	0.084 }	0.046 } (E_{2g})	0.116 }	0.100 }	0.187 }
23	0.025 }	0.035 (A_1)	0.045 (A_1)	0.046 }	−0.001 } (E_u)	0.017 } (E')	0.187 }
22	0.018 (B_1)	0.004 (A_2)	−0.022 } (E_2)	0.039 } (E_{1g})	−0.001 }	0.017 }	0.053 } (E_g)
21	−0.030 (A_1)	−0.024 (A_1)	−0.022 }	0.039 }	−0.027 } (E_g)	−0.006 } (E')	0.053 }
20	−0.061 } (E)	−0.059 (A_1)	−0.051 (B_2)	−0.033 (A_{2u})	−0.027 }	−0.006 }	−0.057 } (T_{1u})
19	−0.061 }	−0.072 (B_1)	−0.085 } (E_1)	−0.018 (B_{2u})	−0.035 (A_{1g})	−0.052 (A_1')	−0.057 }
18	−0.101 (B_2)	−0.096 (B_2)	−0.085 }	−0.102 } (E_{1u})	−0.128 (A_{2u})	−0.095 (A_2'')	−0.058 }
17	−0.182 } (E)	−0.178 (B_2)	−0.189 } (E_3)	−0.102 }	−0.135 (A_{2u})	−0.146 (A_2'')	−0.147 (A_{2u})
16	−0.182 }	−0.189 (A_1)	−0.189 }	−0.119 (B_{1u})	−0.192 (A_{1g})	−0.178 (A_1')	−0.166 (A_{1g})
15	−0.191 (A_1)	−0.192 (A_2)	−0.198 } (E_2)	−0.189 (A_{1g})	−0.203 } (E_g)	−0.195 } (E'')	−0.195 } (T_{2g})
14	−0.205 (B_2)	−0.202 (B_1)	−0.198 }	−0.214 } (E_{2g})	−0.203 }	−0.195 }	−0.195 }
13	−0.206 (A_1)	−0.205 (A_1)	−0.198 (A_1)	−0.214 }	−0.232 (A_{1g})	−0.234 (A_1')	−0.195 }
12	−0.339 } (E)	−0.322 (A_1)	−0.296 (B_2)	−0.221 (A_{1g})	−0.305 } (E_u)	−0.298 } (E')	−0.308 } (T_{1u})
11	−0.339 }	−0.354 (B_1)	−0.381 } (E_1)	−0.290 (A_{2u})	−0.305 }	−0.298 }	−0.308 }
10	−0.392 (B_2)	−0.392 (B_2)	−0.381 }	−0.373 } (E_{1u})	−0.427 (A_{2u})	−0.414 (A_2'')	−0.308 }
9	−0.583 (A_1)	−0.581 (A_1)	−0.573 (A_1)	−0.373 }	−0.559 (A_{1g})	−0.507 (A_1')	−0.478 (A_{1g})
1–8	(inner shells)			−0.558 (A_{1g})			

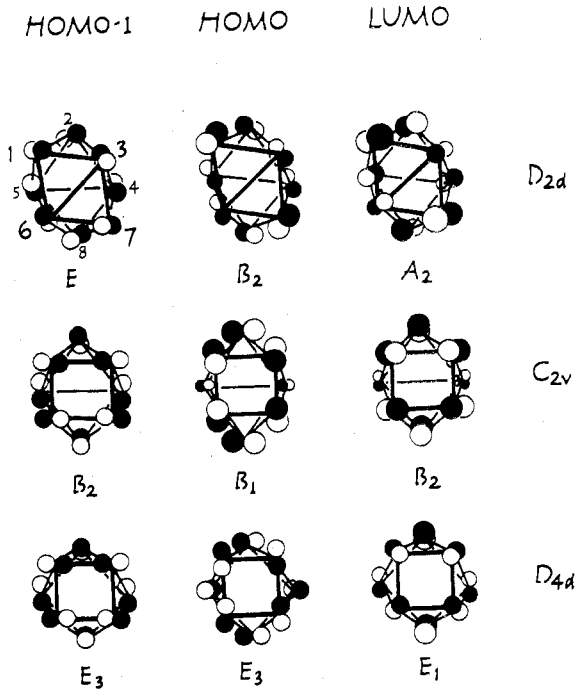

Figure 3. HOMO-1, HOMO, and LUMO for D_{2d}, C_{2v}, and D_{4d} triumvirate. Only the contributions from p orbitals are depicted although there is some hybridization.

change is reflected by a doubling of the overlap population between centers 4 and 5 in the HOMO-1. While the second square is opened, the p_π interaction between centers 4 and 5 is stretched in the HOMO-1 (the p_π–p_π overlap population decreases by a factor of 10) and at the same time p orbitals on centers 2 and 8 are brought into a stronger antibonding arrangement. Thus, the opening of a second face is strongly opposed by the HOMO-1. No such opposition is expressed by the HOMO-1 during the opening of the 1–3–6–7 face of the D_{2d} structure, because the p orbitals on centers 3 and 6 are not in optimal π-bonding relationship and the p orbitals on centers 1 and 7 are not in optimal π-antibonding relationship. Furthermore, because of the lower symmetry along the $D_{2d} \rightleftarrows C_{2v}$ pathway, the molecular orbitals are more flexible and freer to mix in orbitals of like symmetry in order to minimize antibonding relationships.

Population analyses[21,22] for the D_{2d}, C_{2v}, and D_{4d} triumvirate are presented in Table IV. Atomic charges suggest that the order of susceptibility to electrophilic attack is $B_1 = B_2 = B_7 = B_8 > B_3 = B_4 = B_5 = B_6$ for the D_{2d} structure and $B_2 = B_8 > B_1 = B_3 = B_6 = B_7 > B_4 = B_5$ for the C_{2v} structure. These predictions are also consistent with the orders of electrophilic attack predicted on the basis of sums of atomic charges over the eight highest occupied molecular orbitals and on the basis of inner-shell eigenvalues.[24] Thus, the four coordinate borons would also appear to be the most likely sites of ion pairing. This prediction is confirmed in section V.

The overlap populations are clearly consistent with the conclusion that the $D_{2d} \rightarrow C_{2v}$ conversion should be more facile than the $C_{2v} \rightarrow D_{4d}$. In the D_{2d} structure the smallest degree of bonding[22] for near neighbors is between B_3 and B_6 (and the other symmetry-related equatorial bonds). Naturally, this is the bond which breaks in proceeding to the C_{2v} structure. Note, however, that during the $D_{2d} \rightarrow C_{2v}$ transformation the degrees of bonding of the remaining equatorial bonds increase. In particular the degree of bonding of the 4–5 bond increases from 0.331 to 0.390 as the opposite 3–6 bond is opened. Thus, the opening of the 4–5 bond in the C_{2v} structure is expected to be significantly less facile than the opening of the 3–6 bond in the D_{2d} structure and hence the D_{4d} structure is not expected to be energetically competitive with the D_{2d} and C_{2v} structures.

Figure 4 depicts the LMO's for the various structures of high symmetry. All structures are well localized with the exception of the LMO's generated from the full symmetry canonical molecular orbitals (CMO's) of the O_h structure (designated $O_h(O_h)$ in Figure 4). The localized valence orbitals for this localization are barely determinate: the highest eigenvalue for the second derivative matrix[16] is very small and negative for the valence MO's. However, the LMO's obtained from the calculation which was primed by using a converged density matrix from a D_{2d} structure (designated $O_h(D_{2d})$) are well localized and correspond to a well-defined maximum on the localization surface. Furthermore, the separation of LMO centroids is significantly better for the $O_h(D_{2d})$ structure than for the $O_h(O_h)$ structure.

The localized structure for the D_{2d} geometry has the C_2 symmetry reported earlier.[10] In proceeding to the C_{2v} geometry the 3–6 diagonal of the 1–3–7–6 diamond is opened forming a square face. Only modest changes in the LMO structure occur during the diamond-square transformation.[25] The 1–6–3 and 3–7–6 bond orbitals lose their contributions from centers

Table IV. Population Analysis of Wave Functions

Group Charges[a,b]

atom[d]	D_{2d}	C_{2v}	D_{4d}
1	−0.289	−0.249	−0.250
2	−0.289	−0.304	−0.250
3	−0.211	−0.249	−0.250
4	−0.211	−0.198	−0.250
5	−0.211	−0.198	−0.250
6	−0.211	−0.249	−0.250
7	−0.289	−0.249	−0.250
8	−0.289	−0.304	−0.250

Overlap Populations[a]

bond	D_{2d}	C_{2v}	D_{4d}
1-2	0.706	0.588	0.457
1-3	0.397	0.345	0.586
1-5	0.397	0.335	0.457
1-6	0.676	0.805	0.586
1-7	−0.057	−0.002	−0.000
2-4	0.676	0.538	0.586
3-6	0.331	−0.002	0.000
3-4	0.331	0.335	0.457
4-2	0.676	0.538	0.586
4-5	0.331	0.390	0.000

Group Charges (APS)[b,c]

atom	D_{2d}	C_{2v}	D_{4d}
1	−0.305	−0.251	−0.250
2	−0.305	−0.314	−0.250
3	−0.195	−0.251	−0.250
4	−0.195	−0.183	−0.250
5	−0.195	−0.183	−0.250
6	−0.195	−0.251	−0.250
7	−0.305	−0.251	−0.250
8	−0.305	−0.314	−0.250

Degrees of Bonding (APS)[c]

bond	D_{2d}	C_{2v}	D_{4d}
1-2	0.909	0.746	0.623
1-3	0.506	0.426	0.667
1-5	0.506	0.453	0.623
1-6	0.801	0.955	0.667
1-7	0.027	0.109	0.098
2-4	0.801	0.643	0.667
3-6	0.448	0.109	0.098
3-4	0.448	0.453	0.623
4-2	0.801	0.643	0.667
4-5	0.448	0.503	0.098

[a] Group charges and overlap populations from a Mulliken population analysis.[21] [b] Group charges are computed by summing the atomic populations of the designated boron and the terminal hydrogen attached to it. [c] Group charges and degrees of bonding from an Armstrong, Perkins, and Stewart analysis.[22] [d] Atom numbers refer to Figure 1.

3 and 6, respectively, as the square is opened. A second diamond-square transformation, this time opening the 2–4–8–5 diamond, yields a D_{4d} structure with only modest changes in the LMO structure. Twisting the 1–3–7–6 square face of the D_{4d} structure with simultaneous equalization of all nearest neighbor distances yields the O_h geometry. In passing to the O_h geometry the LMO's of the D_{4d} geometry correlate cleanly with the $O_h(D_{2d})$ LMO's. During this transformation all three-center LMO's of the D_{4d} structure correlate with two-center LMO's of the $O_h(D_{2d})$ structure, interaction between the 2–4–8–5 and 1–3–7–6 faces being formally lost in the process. In contrast, no simple correlation can be discerned between the LMO's of the D_{4d} geometry and those of the $O_h(O_h)$ structure.

The LMO patterns for the geometries with D_{6h}, D_{3h}, and D_{3d} symmetry all have the symmetry of the common subgroup, C_{3v}. Furthermore, correlations between the LMO structures

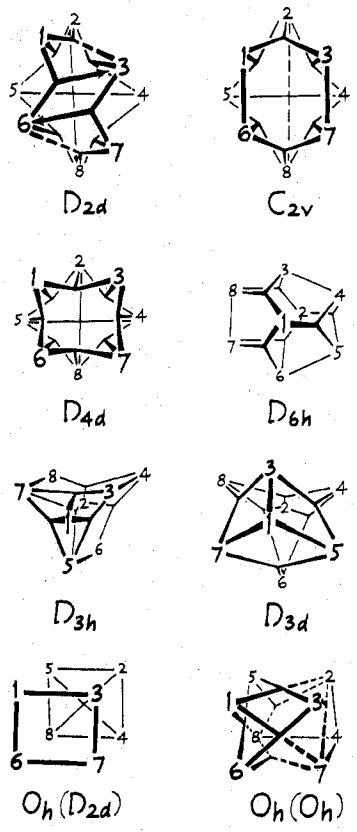

Figure 4. Localized molecular orbitals for structures of high symmetry. Bonding conventions from ref 23 are (1) (- - -) 0.15–0.25 e, (2) (—) 0.25–0.35 e, (3) (- - -) 0.35–0.50 e, and (4) (—) population greater than 0.50 e.

are readily discerned. As the 4–6–8 triangle descends from apex 1 and the 3–5–7 triangle rises from apex 2 the D_{6h} geometry is converted into the D_{3d} geometry. Bonding interactions between apex 1 with triangle 3–5–7 are expected to intensify while those with triangle 4–6–8 are expected to weaken. In keeping with this expectation the 1–3–8, 1–4–5, and 1–6–7 bond orbitals are converted into 1–3, 1–5, and 1–7 two-center orbitals, respectively. An alternative solution is chosen by vertex 2. Here the expected intensification of bonding interactions between vertex 2 and centers 4, 6, and 8 and the expected weakening of interaction with vertices 3, 5, and 7 is accomplished by converting the 2–3–8, 2–4–5, and 2–6–7 LMO's of the D_{6h} structure into 2–4–8, 2–4–6, and 2–6–8 LMO's in the D_{3d} structure. The two triangles remain connected in the D_{3d} structure by conversion of the two-center LMO's of the D_{6h} structure into three-center LMO's, each three-center LMO having two centers in the 3–5–7 triangle and one in the 4–6–8 triangle.

Twisting the upper triangle of the D_{3d} geometry counterclockwise until borons 3, 5, and 7 eclipse borons 4, 6, and 8, respectively, yields the D_{3h} geometry. In so doing the strengthening bond interaction between centers 3 and 4 and the weakening of the bond between centers 4 and 5 is reflected by the conversion of the 3–4–5 three-center orbital into a 3–4 two-center orbital. Simultaneously, the 5–6–7 and 3–7–8 orbitals are converted into 5–6 and 7–8 two-center orbitals. Also, the LMO's in the upper cap rearrange to solve the bonding in that cap by using three-center LMO's rather than the two-center LMO's used in the D_{3d} structure.

V. Environmental Factors

Our calculations are clearly consistent with a fluxional $B_8H_8^{2-}$ ion, the C_{2v} structure serving as a low-energy transitional structure for rearrangement of borons within the more

Table V. Ion Pairing: Relative Energies[a] of Singly and Doubly Lithiated Complexes of $B_8H_8^{2-}$

symmetry	facet lithiated	E,[a] kcal/mol
	A. One Lithium	
D_{2d}	1-2-3 face	0.0
D_{2d}	1-2 edge	1.9
D_{2d}	1-3-6 face	6.4
D_{2d}	3-6 edge	7.0
C_{2v}	1-2-3 face	3.8
C_{2v}	square face	−2.2
D_{4d}	square face	23.9
	B. Two Lithiums	
D_{2d}	1-2 and 7-8 edges	0.0
D_{2d}	1-2-3 and 6-7-8 faces	5.9
D_{2d}	3-6 and 4-5 edges	20.4
C_{2v}	1-2-3 and 6-7-8 faces	9.8
C_{2v}	4-5 edge and square face	15.9
C_{2v}	1-2-3 face and square face	16.7
D_{4d}	square faces	37.6

[a] All geometries have been optimized with respect to lithium positions. The $B_8H_8^{2-}$ geometry was held fixed at the optimum for the given symmetry while the lithium positions were optimized along an axis normal to the given facet and passing through its gravitational center.

stable D_{2d} structure. It has been suggested that solvation or ion pairing might stabilize square faces[2,26] in the C_{2v} and D_{4d} structures and hence change the order of stability. We have attempted to assess the validity of this hypothesis by computing the differential stabilization of the C_{2v} and D_{4d} structures compared with the D_{2d} upon solvation with HF or ion pairing with Li^+. In the case of solvation by HF, PRDDO calculations on the HF + $B_8H_8^{2-}$ supermolecule suggest a very weakly bound complex (binding energy less than 5 kcal/mol) when HF approaches along a normal passing through either the center of the 3-6-7 face or 3-6 edge of the D_{2d} structure or along a normal to the square face of the C_{2v} structure. HF appears to prefer an approach with the HF axis collinear with the normal and the hydrogen closest to the respective face. However, little preferential stabilization is observed for the C_{2v} structure compared with the D_{2d} and, hence, solvation by HF does not appear to significantly stabilize a square face.

PRDDO calculations were also performed on the $Li^+B_8H_8^{2-}$ ion pair (Table V and Figure 1). Due to the strong Coulombic interaction the ion pair is stabilized by over 220 kcal/mol relative to the separated ions. A glance at the charges for the D_{2d} structure in Table IV would suggest that the 1-2 edge and 1-2-3 triangle are the most likely sites for lithiation. The PRDDO calculations on $Li^+B_8H_8^{2-}$ (D_{2d}) confirm this expectation, the 1-2-3 triangle lithiation being preferred over 1-2 edge lithiation by 2 kcal/mol. Lithiation of the C_{2v} structure does seem to stabilize the square face and thus preferentially stabilizes the C_{2v} structure relative to the D_{2d}. The C_{2v} structure, square lithiated, is about 2 kcal/mol more stable than the most stable $Li^+B_8H_8^{2-}$ (D_{2d}) ion pair. However, computations on $Li^+B_8H_8^{2-}$ (D_{4d}) suggest that, while the margin has been reduced, the D_{4d} structure remains significantly less stable than either C_{2v} or D_{2d} (Table V).

While the pairing of a single Li^+ ion with $B_8H_8^{2-}$ does seem to preferentially stabilize structures with square faces, it seems likely that a certain proportion of $B_8H_8^{2-}$ might well be paired with two cations in low dielectric media. When two Li^+ ions are paired with $B_8H_8^{2-}$, the computed interaction energy is about 370 kcal/mol for the D_{2d} structure. However, Coulombic repulsion between the ions appears to alter the preferred sites of lithiation. In particular, lithiation of the equivalent 1-2 and 7-8 edges now appears to be preferred over simultaneous lithiation of the 1-2-3 and 6-7-8 faces (Table V and Figure 1). Furthermore, square faces do not seem to be stabilized when two Li^+ ions pair with the C_{2v} or D_{4d} structure.

Table VI. Optimized B-B Bond Distances in $B_8H_8^{2-}$ Compared with Crystallographic Structure

bond	distance, Å	
	PRDDO	X-ray[a]
1-2	1.569	1.56
2-3	1.768	1.76
1-6	1.630	1.72
6-3	1.849	1.93

[a] Reference 5.

In particular, placement of two Li^+ ions on the 1-2-3 and 6-7-8 faces of the C_{2v} structure appears to be more favorable than the arrangements studied where one of the Li^+ ions is placed on the square face. Furthermore, the most stable dilithiated C_{2v} structure is now 10 kcal/mol above the most stable dilithiated D_{2d} structure studied whereas the separation was about 4 kcal/mol for the naked ions. Thus, an increase in the activation energy for the intramolecular rearrangement may accompany ion pairing by two cations. The situation is even worse for the D_{4d} structure where placement of the ions on the square faces very nearly reestablishes the D_{2d}–D_{4d} separation computed for the naked ions.

Of course, lithium ions are a special case in that some significant covalent interactions with the $B_8H_8^{2-}$ dianion may be operative. Nevertheless, these calculations suggest that where ion pairing is to be expected, the relative stability of structures may be altered in fluxional molecules of the sort studied here. We also comment that no account has been taken here of back-polarization of the medium, which may moderate these Coulomb effects to some extent but probably not change these qualitative conclusions.

VI. Discussion

An X-ray crystallographic structure determination on $Zn(NH_3)_4B_8H_8$ yields D_{2d} symmetry for the B_8 polyhedron,[5,6] consistent with our calculation of the stability of the D_{2d} structure. Optimized bond distances for the D_{2d} structure are compared with the X-ray results in Table VI. The average error in bond distances is 0.04 au, the largest error being 0.09 au for the 1-6 distance. Thus, PRDDO yields a slightly more compact geometry for $B_8H_8^{2-}$ than does the crystal structure.

The ^{11}B nuclear magnetic resonance spectra of $B_8H_8^{2-}$ have been interpreted as arising from the C_{2v} and/or D_{4d} structures, while the D_{2d} structure serves as a higher energy intermediate for facile boron rearrangement.[7] Our calculations are clearly consistent with a fluxional $B_8H_8^{2-}$ ion but predict the D_{2d} structure to be the most stable of the D_{2d}, C_{2v}, and D_{4d} triumvirate. Furthermore, the C_{2v} and D_{4d} structures are not predicted to be thermodynamically stable intermediates. The very small barrier which exists near the terminus of the $D_{2d} \rightarrow C_{2v}$ path (Figure 2) is probably attributable to the idealized nature of the linear synchronous path rather than to the existence of a real barrier along the optimum path.

The NMR spectra were reported in media of widely varying dielectric constant. In water, $Cs_2B_8H_8$ showed a single boron absorption which has been tentatively attributed to the D_{4d} structure.[2] In such a high dielectric, ion pairing may not occur to any significant extent and hence the spectrum in water may be more characteristic of the bare ion than are spectra in media of lower dielectric constant.[27] In view of our calculations reported here on the bare ion, it does not seem reasonable to invoke the D_{4d} structure in order to explain the NMR spectra. An alternative interpretation of the ^{11}B spectrum in water is that it arises from a fluxional D_{2d} structure in which borons are permuted between the two distinct D_{2d} magnetic environments, the C_{2v} geometry serving as a transitional structure for the permutation. For example, opening the 1-3-7-6 face by breaking the 3-6 bond in the D_{2d} structure (Figure 1)

followed by closure of the 1–7 diagonal in the resultant C_{2v} structure leads to a new D_{2d} structure in which borons 3 and 6 have exchanged environments with borons 1 and 7.

The spectra in low dielectric media are much more complex.[2] At low temperatures the ^{11}B spectrum of $Na_2B_8H_8$ in 1,2-dimethoxyethane consists of three doublets[28] of relative intensity 2:4:2 superimposed on a second spectrum consisting of a single doublet. These subspectra have been interpreted[2] as arising from two stable species: the C_{2v} and D_{4d} structures, respectively. In these low dielectrics, ion pairing is quite likely even when counterions as large as tetra-*n*-butylammonium ion are employed.[29] However, the computations discussed in the previous section lead us to conclude that the D_{4d} structure will not be present in any considerable amount even when the square faces are complexed with ions. We leave open the possibility that the C_{2v} structure, complexed with one cation, is more stable than the D_{2d} in low dielectric media. Table V suggests that if a large fraction of the $B_8H_8^{2-}$ dianions is paired with a single lithium cation, the C_{2v} structure lithiated on a square face (ion pair symmetry also C_{2v}) would predominate. However, rough calculations based upon the ion-pairing theory of Fuoss[30] suggest that nearly all dianions will be paired with two cations in low dielectric media ($\epsilon \sim 4$).[31] If this is the case, then the D_{2d} structure paired at the 1–2 and 7–8 edges (ion-pair symmetry also D_{2d}) might be reestablished as the most stable structure. We also should note that the effective symmetry of the D_{2d} dianion could be reduced to C_{2v} without altering the geometry of the anion itself by pairing cations on both the 1–2–3 and 6–7–8 faces.

Several explanations could be put forth to explain the solution NMR spectra but any explanation invoking a stable D_{4d} structure would seem tenuous in view of the present calculations.[32] As an alternative we suggest that equilibria among various ion-paired structurites[34] might account for the NMR spectra in low dielectric media. Such temperature-dependent ion-pairing equilibria have precedent. For example, there are three different ion pairs of $Co(CO)_4^-$ in tetrahydrofuran.[34] Different modes of ion pairing of the octaborane dianion might alter the barrier to internal rearrangement, so that at a given temperature two species might be observed, one whose spectrum is frozen on the NMR time scale (giving rise to the 2:4:2 pattern) and another whose spectrum is a simple doublet. Of course, the observation of separate patterns in the NMR spectrum requires a relatively large free energy of activation ($\gtrsim$20 kcal/mol) for conversion of the two species. Such a barrier is conceivable for the conversion of an ion pair to an ion triplet

$$M(SOL)^+ + MB_8H_8^- + M_2B_8H_8 + SOL$$

where SOL is a solvent molecule. Since large entropy changes are expected to accompany ion pairing, the above scenario might account for the large entropy differences observed between the two species.[32] In the case of the Li^+ cation, Table V clearly eliminates the D_{4d} structure for the $B_8H_8^{2-}$ moiety in both the ion pair and ion triplet while the C_{2v} and D_{2d} structures remain energetically competitive. However, ion pairing with the tetraalkylammonium cation may not give such a large effect.

There are undoubtedly other explanations of the NMR spectra which do not invoke a stable D_{4d} structure. In order to establish conclusively the nature of the species present in solutions of octaborane dianion, more experimental work is needed. In particular, it would be very interesting to do conductivity studies to determine the extent of ion pairing and it might also be profitable to use shift reagents as counterions to elucidate the sites of ion pairing.

Acknowledgment. We thank the National Science Foundation (Grant CHE 77-19899) for support. We would also like to thank Thomas A. Halgren for thoughtful comments.

Notes Added in Proof. Double-ζ calculations recently performed by us on the D_{2d}, C_{2v}, and D_{4d} structures leave unchanged the relative stability order within the triumvirate. Relative to the most stable D_{2d} structure, the C_{2v} and D_{4d} structures lie at 6.6 and 29.7 kcal/mol, respectively (cf. Table I). Details are forthcoming in a future publication.

We also add that M. J. S. Dewar and M. L. McKee, *Inorg. Chem.*, **17**, 1569 (1978), find by the MNDO method that the D_{2d} structure is most stable and that the C_{2v} and D_{4d} structures are less stable by 2 and 21 kcal/mol, respectively.

Registry No. $B_8H_8^{2-}$, 12430-13-6; $Li^+B_8H_8^{2-}$, 69277-71-0; $Li_2^+B_8H_8^{2-}$, 69277-72-1.

References and Notes

(1) (a) Williams College. (b) Harvard University.
(2) E. L. Muetterties, R. J. Wiersema, and M. F. Hawthorne, *J. Am. Chem. Soc.*, **95**, 7520 (1973).
(3) E. I. Tolpin and W. N. Lipscomb, *J. Am. Chem. Soc.*, **95**, 2384 (1973).
(4) D. A. Kleier, D. A. Dixon, and W. N. Lipscomb, *Inorg. Chem.*, **17**, 166 (1978).
(5) L. J. Guggenberger, *Inorg. Chem.*, **8**, 2771 (1969).
(6) F. Klanberg, D. R. Eaton, L. J. Guggenberger, and E. L. Muetterties, *Inorg. Chem.*, **6**, 1271 (1967).
(7) E. L. Muetterties, *Tetrahedron*, **30**, 1595 (1974).
(8) R. Hoffmann and W. N. Lipscomb, *J. Chem. Phys.*, **36**, 2179 (1962).
(9) E. L. Muetterties and B. F. Beier, *Bull. Soc. Chim. Belg.*, **84**, 397 (1975).
(10) D. A. Dixon, D. A. Kleier, T. A. Halgren, J. H. Hall, and W. N. Lipscomb, *J. Am. Chem. Soc.*, **99**, 6226 (1977).
(11) T. A. Halgren and W. N. Lipscomb, *J. Chem. Phys.*, **58**, 1569 (1973).
(12) T. A. Halgren, D. A. Kleier, J. H. Hall, Jr., L. D. Brown, and W. N. Lipscomb, *J. Am. Chem. Soc.*, **100**, 6595 (1978).
(13) E. Switkes, R. M. Stevens, W. N. Lipscomb, and M. D. Newton, *J. Chem. Phys.*, **51**, 2085 (1969).
(14) S. F. Boys, *Rev. Mod. Phys.*, **32**, 306 (1960); S. F. Boys in "Quantum Theory of Atoms, Molecules and the Solid State", P. O. Löwdin, Ed., Academic Press, New York, 1966.
(15) C. Edmiston and K. Ruedenberg, *Rev. Mod. Phys.*, **35**, 457 (1963).
(16) D. A. Kleier, T. A. Halgren, J. H. Hall, and W. N. Lipscomb, *J. Chem. Phys.*, **61**, 3905 (1974).
(17) T. A. Halgren and W. N. Lipscomb, *Chem. Phys. Lett.*, **49**, 225 (1977).
(18) By "transitional structure" we imply either an intermediate or a transition state. We note, however, that while the C_{2v} structure may serve as a transition state for rearrangement of borons in the D_{2d} structure, symmetry restrictions (J. W. McIver, *Acc. Chem. Res.*, **7**, 72 (1974)) would prevent the D_{2d} structure from serving in the same capacity if C_{2v} were the ground-state geometry. Thus, while a synchronous transit pathway connecting D_{2d} structures traverses a C_{2v} structure at the halfway point, the synchronous transit pathway connecting two C_{2v} structures traverses a structure having C_s symmetry.
(19) This appears to be an example of a Hartree–Fock instability of the first type[20] and is usually associated with the existence of a state below that of the symmetry-restricted Hartree–Fock state. A similar instability has been reported for O_2^{2-} in ref 20.
(20) G. Chambaud, B. Levy, and P. Millie, *Theor. Chim. Acta*, **48**, 103 (1978).
(21) R. S. Mulliken, *J. Chem. Phys.*, **23**, 1833 (1955).
(22) D. R. Armstrong, P. G. Perkins, and J. J. P. Stewart, *J. Chem. Soc., Dalton Trans.*, 838 (1973).
(23) J. H. Hall, D. A. Dixon, D. A. Kleier, T. A. Halgren, L. D. Brown, and W. N. Lipscomb, *J. Am Chem. Soc.*, **97**, 4202 (1975).
(24) For the D_{2d} structure the sum over the highest eight valence MO's gives a population of 2.09 and 1.91 electrons on BH groups 1 and 3, respectively, while the corresponding eigenvalues for inner shells are −7.08 and −7.12 au. For the C_{2v} structure the sum over the highest eight occupied MO's gives populations of 2.03, 2.08, and 1.87 electrons for BH groups 1, 2, and 4, respectively, and inner-shell eigenvalues of −7.09, −7.08, and −7.12 au.
(25) Two different localized structures were observed at R = 0.0, 0.2, 0.4, and 0.6 along the $D_{2d} \rightleftarrows C_{2v}$ synchronous transit pathway corresponding to multiple maxima on the localization surface. The alternative LMO structure for the D_{2d} geometry was obtained as the last of a series of 13 localizations using randomized starting MO's. It possesses C_s symmetry and is depicted below.

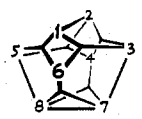

The structure depicted in Figure 1 is better localized as judged by the separation of LMO centroids.
(26) We note that square faces have been observed for B_{12} polyhedra in crystals of UB_{12} (F. Bertaut and P. Blum, *C.R. Hebd. Seances Acad. Sci.*, **229**,

666 (1949)) and ZrB_{12} (B. Post and F. W. Glaser, *J. Met.* **4**, 631 (1952)).
(27) Of course, the polar solvent may have some effect on the stability of the various structures, but our computations using HF as a model for a polar solvent molecule suggests that the effect may be rather small.
(28) The doublet splitting arises from coupling with terminal hydrogens.
(29) R. M. Fuoss and C. A. Kraus, *J. Am. Chem. Soc.*, **79**, 3304 (1957).
(30) R. M. Fuoss, *J. Am. Chem. Soc.*, **80**, 5059 (1958).
(31) For example, if one considers ion pairing between Na^+ and $NaB_8H_8^-$ in diethyl ether (ϵ 4.34) at 25 °C and assumes ionic radii of 0.95 and 3.0 Å for the cation and anion, respectively, the fraction of ions associated is predicted to be well over 99%.
(32) Our calculations not only place the energy of the D_{4d} structure significantly above the D_{2d} or C_{2v} but also fail to place the D_{4d} structure at a relative minimum. The more open D_{4d} structure could have some entropic stabilization but probably not more than a few to 10 cal/(K mol), but even this stabilization would not give relative stability for D_{4d} at room temperature. An estimate of the entropy difference between the two solution-state forms observed by NMR[2] can be obtained by assuming concentration ratios of 95:5 at −32 °C and 5:95 at 46 °C. This assumption yields ΔH° = 13 kcal/mol and ΔS° = 45 cal/(K mol). Although this ΔH° value is consistent with a previous estimate,[33] this large ΔS° value seems inconsistent with simple face opening and may indicate some form of ion pairing with concomitant loss of freedom and desolvation of ions. This large entropy change further supports our arguments based upon energetic calculations in making less likely the occurrence of the D_{4d} structure as a stable intermediate.
(33) E. L. Muetterties, E. L. Hoel, C. G. Salentine, and M. F. Hawthorne, *Inorg. Chem.*, **14**, 950 (1975).
(34) W. F. Edgell, S. Hegde, and A. Barbetta, *J. Am. Chem. Soc.*, **100**, 1406 (1978).

Contribution from the Department of Chemistry,
National Tsing Hua University, Hsinchu, Taiwan, Republic of China

Symmetry and Isomer Concepts in the Evaluation of Statistical Factors

CHUNG-SUN CHUNG

Received July 13, 1978

Symmetry and isomer concepts are considered in the general evaluation of statistical factors in coordination reactions. If A and B are different monodentate ligands and all of the $(N - n)$B's in the reagent and all of the $(n + 1)$A's in the product of the reaction $MA_nB_{N-n} + A = MA_{n+1}B_{N-n-1} + B$ are structurally or energetically equivalent, the sum of the symmetry and isomer effects of this reaction is equal to $R \ln [(N - n)/(n + 1)] + C$, the statistical factor obtained by the Brönsted method, where C is a constant for the difference in the symmetry of the free ligands, A and B. If the B's in the reagent are not structurally or energetically equivalent, and all of the A's in the product are structurally or energetically equivalent, the sum of the symmetry and isomer effects of this reaction is smaller than $R \ln [(N - n)/(n + 1)] + C$. If the A's in the product are not structurally or energetically equivalent, and all of the B's in the reagent are structurally or energetically equivalent, the sum of the symmetry and isomer effects of this reaction is larger than $R \ln [(N - n)/(n + 1)] + C$.

I. Introduction

Statistical factors have long been used in correlating ionization constants of acids,[1,2] rate constants,[3] and stability constants of metal complexes.[4,5] Benson[3] termed the earlier statistical factors "the intuitive Brönsted method" and showed that the symmetry corrections derived from statistical mechanics can be equivalent to those obtained by this intuitive method. This is true only if there are no isomers present in the system. It is shown in the present work that, when isomers are present, the statistical factor is the sum of the symmetry effect and the isomer effect. Although the statistical factors in current use[6] are satisfactory for monodentate ligands when no isomers are present, this is not the case for octahedral or square-planar complexes to which the factors are frequently applied unless there is no preference for cis or trans positions. Two recent papers[7,8] also pointed out that the Brönsted method for obtaining statistical factors is not general. For polydentate ligands the attempt by Sen[9] to extend the Brönsted method is unsatisfactory because of his oversimplifications. In general, it is necessary to consider the isomer effect to give the correct evaluation of statistical factors. The term "symmetry and isomer effects or contributions" stands for the longer phrase "the entropy change owing to symmetry and isomer effects" in this paper.

II. Theory

The symmetry number σ "is the number of nonequivalent ways in which the atoms of the molecule can be interchanged by rigid rotation of the molecule in space and remain completely indistinguishable from some other such orientational rearrangement".[10] If a complex M(ABC...) has a coordination number N and has N different ligands, then there are $N!$ arrangements of the ligands in the complex. The isomer number r is the total number of geometric and optical isomers of the complex. The isomers (in toto) of M(ABC...) can be rotated to give the $N!$ possible arrangements. The number of rotational operations needed, for each isomer considered separately, equals the symmetry number for MA_N, provided the coordination number and geometry of MA_N and M(ABC...) are the same. Thus

$$r_{M(ABC...)}\sigma_{MA_N} = N! \tag{1}$$

A compound which has no geometric or optical isomers is defined as type I and can have the general formula $M(A_aB_bC_c...)$. The total number of ways to arrange aA, bB, and cC around the central atom is $N!/(a!b!c!...)$. In this case r = 1 by definition. The single isomer can be rotated to obtain the total number of arrangements, and the number of rotational operations needed equals $\sigma_{MA_N}/\sigma_{MA_aB_bC_c...}$, where again N is the same for MA_N and for $MA_aB_bC_c...$ and the geometry is the same. Therefore

$$\frac{N!}{a!b!c!...} = \frac{\sigma_{MA_N}}{\sigma_{MA_aB_bC_c...}} \tag{2}$$

and from eq 1 it follows that

$$r_{M(ABC...)}\sigma_{MA_aB_bC_c} = a!b!c!... \tag{3}$$

Consider the reaction in eq 4, where A and B are mono-

$$MA_nB_{N-n} + A \rightleftharpoons MA_{n+1}B_{N-n-1} + B \tag{4}$$

dentate groups and the structure and coordination number remain unchanged. The symmetry effect of the reaction, ΔS^{sym}, is

$$\Delta S^{sym} = -R \ln \frac{\Pi\sigma_{products}}{\Pi\sigma_{reactants}} \tag{5}$$

When eq 3 is used for the symmetry number for type I compounds, eq 6 is obtained, where C is a constant for the

0020-1669/79/1318-1318$01.00/0